Throughput and Ergodic Capacity of Wireless Energy Harvesting Based DF Relaying Network

Ali A. Nasir, Xiangyun Zhou, Salman Durrani, and Rodney A. Kennedy
Emails: ali.nasir@anu.edu.au, xiangyun.zhou@anu.edu.au, salman.durrani@anu.edu.au, and rodney.kennedy@anu.edu.au

***Abstract*—In this paper, we consider a decode-and-forward (DF) relaying network based on wireless energy harvesting. The energy constrained relay node first harvests energy through radio-frequency (RF) signals from the source node. Next, the relay node uses the harvested energy to forward the decoded source information to the destination node. The source node transfers energy and information to the relay node through two mechanisms, i) time switching-based relaying (TSR) and ii) power splitting-based relaying (PSR). Considering wireless energy harvesting constraint at the relay node, we derive the exact analytical expressions of the achievable throughput and ergodic capacity of a DF relaying network for both TSR and PSR schemes. Through numerical analysis, we study the throughput performance of the overall system for different system parameters, such as energy harvesting time, power splitting ratio, and signal-to-noise-ratio (SNR). In particular, the throughput performance of the PSR scheme outperforms the throughput performance of the TSR scheme for a wide range of SNRs.**

I. Introduction

Recently, energy harvesting through wireless radio frequency (RF) signals has received significant attention [1], [2]. In wireless energy harvesting, ambient RF radiation is captured by the receiver antennas and converted into a direct current (DC) voltage through appropriate circuits [1]. The majority of the recent research in wireless energy harvesting and information processing has considered point-to-point communication systems and studied rate-energy trade-off assuming single-input-single-output (SISO) [1], [3], single-input-multiple-output (SIMO) [4], and multiple-input-multiple-output (MIMO) [5], [6] setups. The application of wireless energy harvesting to orthogonal frequency division multiplexing (OFDM) [7] and cognitive radio [2] based systems has also been considered. Energy beamforming through wireless energy harvesting has been studied for the multi-antenna wireless broadcasting system in [8]. Moreover, secure transmission in the presence of eavesdropper under wireless energy harvesting constraint has been studied in MISO beamforming systems [9].

An important application of wireless energy harvesting is in cooperative relaying networks, where an intermediate relay node assists in the transmission of the source information to the destination. The relay node may have limited battery reserves and thus relies on some external charging mechanism in order to remain active in the network [10]. Therefore, energy harvesting in such networks is particularly important as it can enable information relaying. Some studies have recently considered energy harvesting through RF signals in wireless relaying networks [11]–[16]. The different rate-energy trade-offs to achieve the optimal source and relay precoding in a MIMO relay system is studied in [11]. The outage performance of a typical cooperative communication system is studied in [12]. However, the authors in [11], [12] assume that the relay has its own internal energy source and does not need external charging. Multi-user and multi-hop systems for simultaneous information and power transfer are investigated in [13]. However, the optimization strategy in [13] assumes that the relay node is able to decode information and extract power simultaneously, which, as explained in [1], may not hold in practice. The outage performance of an amplify-and-forward (AF) relaying network under energy harvesting constraints is studied in [14], [15]. For a decode-and-forward (DF) relaying network, the power allocation strategies and outage performance under energy harvesting constraints is studied in [16]. It must be noted that the throughput analysis in DF relaying networks is fundamentally different from the analysis in AF relaying networks under wireless energy harvesting constraint, due to the different nature of the relaying protocols.

In this paper, we consider a DF relaying network and analyze the system throughput in the presence of energy harvesting constraints. We assume that the relay is an energy constrained node and thus harvests energy from the RF signal broadcasted by the source node. Unlike [13], we adopt time switching (TS) and power splitting (PS) receiver architectures proposed in [1], for separate information processing and energy harvesting at the relay node. In time switching-based relaying (TSR), the relay switches in time between energy harvesting and information processing, however, in power splitting-based relaying (PSR), the relay splits the received power for energy harvesting and information processing. Unlike [16], where the outage probability is analyzed in delay-limited transmission mode, we consider the delay-tolerant transmission mode. This implies that the destination node can buffer the received information blocks and can tolerate the delay in decoding the received signal. Thus, the code length can be kept very large compared to the transmission block time. Consequently, we analyze the ergodic capacity of a DF relaying network in the presence of wireless energy harvesting constraint. The main contributions of this work are as summarized below:

- We derive the closed-form analytical expressions for the ergodic capacity and achievable throughput of a DF relaying network in the presence of wireless energy harvesting constraints for both the TSR and the PSR schemes. The derived expressions provide practical design insights into the effect of various parameters on the system performance.
- Using our derived results, we compare the throughput performance of the TSR and PSR schemes for different system parameters, such as, energy harvesting time, power splitting ratio, or signal-to-noise-ratio (SNR). In particular, we show that the throughput performance of the PSR scheme outperforms that of the TSR scheme for a wide range of SNRs.

The rest of the paper is organized as follows. Section II presents the overall system model and assumptions. Sections III

The authors are with Research School of Engineering, The Australian National University, Canberra, Australia. This research was supported under Australian Research Council's Discovery Projects funding scheme (project number DP140101133).

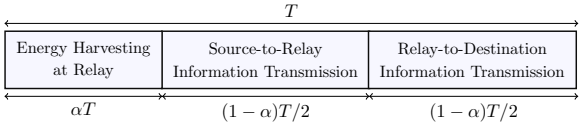

Fig. 1: Transmission block structure in the TSR scheme for energy harvesting and information processing.

and IV detail the analytical derivation of the ergodic capacity and achievable throughput for the TSR and the PSR schemes, respectively. Section V presents the numerical results from which various design insights are obtained. Finally, Section VI concludes the paper.

II. System Model

We consider a DF relaying cooperative network, where the information is transferred from the source node, $\mathbb{S}$, to the destination node, $\mathbb{D}$, through an energy constrained intermediate relay node, $\mathbb{R}$. All nodes are equipped with a single antenna. We assume no direct link between the source and the destination node. Thus, an intermediate DF relay assists the transmission of the source messages to the destination. First, the DF relay harvests energy from the source signal. Then, it uses the harvested energy as a source of transmit power to forward the source information to the destination. We assume that the processing power required by the information decoding circuitry at the relay is negligible as compared to the power used for signal transmission from the relay to the destination. This is justifiable when the transmission distances are large such that the energy transmitted is the dominant source of energy consumption [1], [10]. Throughout this paper, inter-node distances between $\mathbb{S} \rightarrow \mathbb{R}$ and $\mathbb{R} \rightarrow \mathbb{D}$ are denoted by d_1 and d_2, respectively.

The $\mathbb{S} \rightarrow \mathbb{R}$ and $\mathbb{R} \rightarrow \mathbb{D}$ channel gains, denoted by h and g, respectively, are modeled as block-fading and frequency non-selective parameters. The channel is constant over the *block time* T and independent and identically distributed from one block to the next. The fading is assumed to be frequency non-selective Rayleigh block fading. The use of such channels is motivated by prior research in this field [1], [3], [5], [10]–[12], [14], [16]. In this paper, we assume no availability of channel state information (CSI) at the source node. The CSI is only available at the relay and destination receivers, which is inline with the previous work in this research field [11], [12], [14], [16]

For the joint task of energy harvesting and information processing at the relay node, we adopt time switching and power splitting based receiver architectures [1] at the relay node. The detailed analysis of the achievable throughput in the presence of wireless energy harvesting for the time switching and power splitting-based relaying schemes is given in the following sections.

III. Time Switching-Based Relaying (TSR)

Fig. 1 depicts the transmission block structure in the TSR scheme for energy harvesting and information processing at the relay. In Fig. 1, T is the block time in which the information is transmitted from the source node to the destination node and $\alpha \in (0, 1)$ denotes the fraction of the block time in which the relay harvests energy from the source signal. The remaining block time, $(1 - \alpha)T$, is used for information transmission in such a way that half of that, $(1 - \alpha)T/2$, is used for the source to relay information transmission and the remaining half, $(1 - \alpha)T/2$, is used for the relay to destination information transmission. The relay consumes all the harvested energy while forwarding the source signal to the destination. The choice of the time fraction, α, controls the achievable throughput at the destination. The following subsections analyze the energy harvesting and information processing at the relay node.

A. $\mathbb{S} \rightarrow \mathbb{R}$ Energy Harvesting and Information Transmission

The received baseband signal at the relay node, $y_r(k)$, is given by [1]

$$y_r(k) = \frac{1}{\sqrt{d_1^m}}\sqrt{P_s}hs(k) + n_{a,r}(k) + n_{c,r}(k), \tag{1}$$

where $k = 1, 2, \ldots$ denotes the symbol index, h is the source to relay channel gain, d_1 is the source to relay distance, P_s is the transmitted power from the source, m is the path loss exponent, and $s(k)$ is the kth normalized information symbol from the source, i.e., $\mathbb{E}\{|s(k)|^2\} = 1$, $\mathbb{E}\{\cdot\}$ is the expectation operator, $|\cdot|$ is the absolute value operator, $n_{a,r}(k)$ is the baseband additive white Gaussian noise (AWGN) introduced by the receiving antenna at the relay node and $n_{c,r}(k)$ is the AWGN due to radio frequency (RF) band to baseband signal conversion.

As shown in Fig. 1, the received RF signal at the relay node is first sent to the *energy harvesting receiver* (for αT time) and then to the *information receiver* (for $(1 - \alpha)T/2$ time). The energy harvesting receiver rectifies the RF signal directly and gets the direct current to charge up the battery. The details of such an energy harvesting receiver can be found in [1]. Using (1), the harvested energy, E_h^{TS} during energy harvesting time αT is given by [1]

$$E_h^{\text{TS}} = \frac{\eta P_s |h|^2}{d_1^m}\alpha T, \tag{2}$$

where $0 < \eta < 1$ is the energy conversion efficiency which depends on the rectification process and the energy harvesting circuitry [1].

B. $\mathbb{R} \rightarrow \mathbb{D}$ Information Transmission

After the source to relay information transmission, the DF relay decodes the source signal and forward it to the destination node with the power P_r^{TS}, which is available from the energy harvested during energy harvesting time. The received signal at the destination node, $y_d^{\text{TS}}(k)$, in the TSR scheme is given by

$$y_d^{\text{TS}}(k) = \frac{1}{\sqrt{d_2^m}}\sqrt{P_r^{\text{TS}}}g\bar{s}(k) + n_{a,d}(k) + n_{c,d}(k), \tag{3}$$

where d_2 is the relay to destination distance, g is the relay to destination channel gain, $\bar{s}(k)$ is the decoded version of the signal $s(k)$, and $n_{a,d}(k)$ and $n_{c,d}(k)$ are the antenna and conversion AWGNs at the destination node, respectively. Since relay node transmits the decoded signal $\bar{s}(k)$ using the harvested energy E_h^{TS} as a source of power, for $(1-\alpha)T/2$ time, the transmitted power from the relay node, P_r^{TS}, can be given by

$$P_r^{\text{TS}} = \frac{E_h^{\text{TS}}}{(1-\alpha)T/2} = \frac{2\eta P_s |h|^2 \alpha}{d_1^m(1-\alpha)}. \tag{4}$$

Substituting the value of P_r^{TS} from (4) into (3), the received signal at the destination, $y_d^{\text{TS}}(k)$ in terms of P_s, η, α, d_1 and d_2, is given by

$$y_d^{\text{TS}}(k) = \frac{\sqrt{2\eta P_s |h|^2 \alpha} g \bar{s}(k)}{\sqrt{d_1^m d_2^m (1-\alpha)}} + n_d(k), \tag{5}$$

where $n_d(k) \triangleq n_{a,d}(k) + n_{c,d}(k)$ is the overall AWGN at the destination node.

C. Throughput Analysis

Using (1), the SNR at the relay node, γ_r^{TS}, in the TSR scheme is given by

$$\gamma_r^{\text{TS}} = \frac{P_s |h|^2}{d_1^m \sigma^2_{n_r^{\text{TS}}}}, \tag{6}$$

where $\sigma^2_{n_r^{\text{TS}}} \triangleq \sigma^2_{n_{a,r}} + \sigma^2_{n_{c,r}}$ is the variance of overall AWGN at the relay node, $n_r^{\text{TS}} \triangleq n_{a,d}(k) + n_{a,c}(k)$, in the TSR scheme and $\sigma^2_{n_{a,r}}$ and $\sigma^2_{n_{c,r}}$ are the noise variances of the AWGNs $n_{a,d}(k)$ and $n_{c,d}(k)$. Using (5), the SNR at the destination, γ_d^{TS}, in the TSR scheme is given by

$$\gamma_d^{\text{TS}} = \frac{2\eta P_s |h|^2 |g|^2 \alpha}{d_1^m d_2^m \sigma^2_{n_d} (1-\alpha)}, \tag{7}$$

where $\sigma^2_{n_d} \triangleq \sigma^2_{n_{a,d}} + \sigma^2_{n_{c,d}}$. In order to determine the throughput, we need to evaluate the ergodic capacity for source to relay link, C_r^{TS}, and for relay to destination link, C_d^{TS}. Using the received SNRs, γ_r^{TS} and γ_d^{TS}, defined in (6) and (7), respectively, C_r^{TS} and C_d^{TS} are given by

$$C_r^{\text{TS}} = \mathbb{E}_h \left\{ \log_2(1+\gamma_R^{\text{TS}}) \right\} \ , \ C_d^{\text{TS}} = \mathbb{E}_{h,g} \left\{ \log_2(1+\gamma_D^{\text{TS}}) \right\} \tag{8}$$

where γ_R^{TS} depends on h and γ_D^{TS} depends on h and g. Note that we need to calculate the ergodic capacities for both source to relay and relay to destination links because the actual ergodic capacity is given by the minimum of C_r^{TS} and C_d^{TS} [17]. The analytical expressions for the ergodic capacities, C_r^{TS} and C_d^{TS}, are given in the following theorem.

Theorem 1. *The ergodic capacities, C_r^{TS} and C_d^{TS} for the TSR scheme are given by*

$$C_r^{TS} = \frac{\lambda_h e^{\frac{a}{\lambda_h}} E_1\left(\frac{a}{\lambda_h}\right)}{a \log(2)} \tag{9a}$$

$$C_d^{TS} = -\frac{2b}{\lambda_g \lambda_h \log(4)} G^{m,n}_{p,q}\left(\begin{array}{c} [\{0\},\{\}] \\ [\{-1,0,0\},\{\}] \end{array} \middle| \frac{b}{\lambda_g \lambda_h} \right) \tag{9b}$$

where $a \triangleq \frac{d_1^m \sigma^2_{n_r^{TS}}}{P_s}$, $E_1(x) = \int_x^\infty \frac{e^{-t}}{t} dt$ is the exponential integral, λ_h and λ_g are the mean values of the exponential random variables $|h|^2$ and $|g|^2$, respectively, log *is the natural logarithm, $b \triangleq \frac{d_1^m d_2^m \sigma^2_{n_d}(1-\alpha)}{2\eta P_s \alpha}$ and the meijerG function is defined below*

$$G^{m,n}_{p,q}\left(\begin{array}{c} [\{a_1,\ldots,a_m\},\{a_{m+1},\ldots a_p\}] \\ [\{b_1,\ldots,b_n\},\{b_{n+1},\ldots b_q\}] \end{array} \middle| z \right) = \frac{1}{2\pi\iota} \int \frac{\prod_{j=1}^m \Gamma(1-a_j-s) \prod_{j=1}^n \Gamma((b_j+s)}{\prod_{j=m+1}^p \Gamma(a_j+s) \prod_{j=n+1}^q \Gamma((1-b_j-s)} z^{-s} ds, \tag{10}$$

where $\iota = \sqrt{-1}$ and $\Gamma(x) = \int_0^\infty t^{x-1} e^{-t} dt$ is the Gamma function.

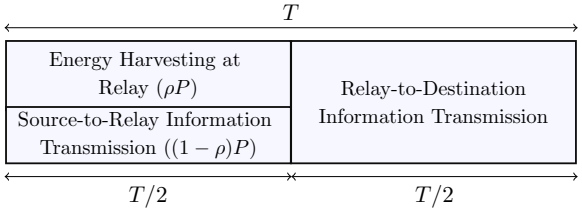

Fig. 2: Transmission block structure in the PSR scheme for energy harvesting and information processing.

Proof: The proof is given in Appendix A. ∎

Using (9), the ergodic capacity of the TSR scheme, C^{TS}, is given by

$$C^{\text{TS}} = \min\left\{C_r^{\text{TS}}, C_d^{\text{TS}}\right\} \tag{11}$$

Given that $(1-\alpha)T/2$ is the effective communication time from the source node to the destination node in the block of time T seconds and if source transmits at a fixed rate equal to the ergodic capacity, i.e., C^{TS} bits/sec/Hz, the throughput, τ^{TS} of the TSR scheme is given by

$$\tau^{\text{TS}} = \frac{(1-\alpha)T/2}{T} C^{\text{TS}} = \frac{1-\alpha}{2} \min\left\{C_r^{\text{TS}}, C_d^{\text{TS}}\right\}, \tag{12}$$

where the throughput, τ^{TS} in (12) depends on P_s, η, α, d_1, d_2, $\sigma^2_{n_r^{\text{TS}}}$ and $\sigma^2_{n_d}$. It is desirable to find the optimal value of α, that result in the maximum value of throughput, τ^{TS}. Since, the analytical expression of τ^{TS} involves complex meijerG function, which in turn depends on α, it seems intractable to evaluate the closed-form expressions for the optimal value of α in terms of τ. However, the optimization can be done offline by numerically evaluating the optimal values of α for the given system parameters, P_s, η, d_1, d_2, $\sigma^2_{n_r^{\text{TS}}}$ and $\sigma^2_{n_d}$.

IV. Power Splitting-Based Relaying (PSR)

Fig. 2 shows the transmission block structure in the PSR scheme for energy harvesting and information processing at the relay, where P is the received signal power and T is the block time. Half of the time, $T/2$ is used for the source to relay information transmission and the remaining half, $T/2$ is used for the relay to destination information transmission. During the first half, the fraction of the received signal power, ρP is used for energy harvesting and the remaining received power, $(1-\rho)P$ is used for transmitting source information to the relay node, where $\rho \in (0,1)$. In PSR scheme, the choice of the power fraction, ρ controls the achievable throughput at the destination. The following subsections analyze the energy harvesting and information processing at the relay for the PSR scheme.

A. $\mathbb{S} \to \mathbb{R}$ Energy Harvesting and Information Transmission

In the PSR scheme, the power splitter at the relay node splits the received signal in $\rho : 1-\rho$ proportion, such that the portion of the received signal, $\sqrt{\rho} y_r(k)$ is sent to the energy harvesting receiver and the remaining signal strength, $\sqrt{1-\rho} y_r(k)$ drives the information receiver, where $y_r(k)$ is defined in (1),. Using the signal received at the input of the energy harvesting receiver, $\sqrt{\rho} y_r(k) = \frac{1}{\sqrt{d_1^m}} \sqrt{\rho P_s} h s(k) + \sqrt{\rho} \sqrt{\rho} n_{a,r}(k)$, the harvested energy, E_h^{TS} at the relay in the PSR scheme is given by [1]

$$E_h^{\text{PS}} = \frac{\eta \rho P_s |h|^2}{d_1^m}(T/2), \tag{13}$$

where the energy is harvested at the relay during half of the block time, $T/2$, as shown in Fig. 2, and $0 < \eta < 1$ is the energy conversion efficiency. After power splitting, the baseband signal at the input of the information receiver, $\sqrt{1-\rho}y_r(k)$, in the PSR scheme is given by

$$\sqrt{1-\rho}y_r(k) = \frac{1}{\sqrt{d_1^m}}\sqrt{(1-\rho)P_s}hs(k) + \sqrt{(1-\rho)}n_{a,r}(k) + n_{c,r}(k). \tag{14}$$

B. $\mathbb{R} \rightarrow \mathbb{D}$ Information Transmission

Using the received signal, $\sqrt{1-\rho}y_r(k)$ in (14), the DF relay decodes the source signal and forward it to the destination node with the power P_r^{PS}, which is available from the energy harvested during the first half of the block time T. The received signal at the destination node, $y_d^{\text{PS}}(k)$, in the PSR scheme is given by

$$y_d^{\text{PS}}(k) = \frac{1}{\sqrt{d_2^m}}\sqrt{P_r^{\text{PS}}}g\bar{s}(k) + n_{a,d}(k) + n_{c,d}(k), \tag{15}$$

where the transmitted power from the relay node, P_r^{PS}, can be given by

$$P_r^{\text{PS}} = \frac{E_h^{\text{PS}}}{T/2} = \frac{\eta P_s |h|^2 \rho}{d_1^m}. \tag{16}$$

Substituting the value of P_r^{PS} from (16) into (15), the received signal at the destination, $y_d^{\text{PS}}(k)$ in terms of P_s, η, α, d_1 and d_2, is given by

$$y_d^{\text{PS}}(k) = \frac{\sqrt{\eta P_s |h|^2 \rho}gs(k)}{\sqrt{d_1^m d_2^m}} + n_d(k). \tag{17}$$

C. Throughput Analysis

Given the received signal at the input of the information receiver at the relay node, $\sqrt{1-\rho}y_r(k)$ in (14), the SNR at the relay node, γ_r^{PS}, in the PSR scheme is given by

$$\gamma_r^{\text{PS}} = \frac{P_s^2 |h|^2 (1-\rho)}{d_1^m \sigma^2_{n_r^{\text{PS}}}}, \tag{18}$$

where $\sigma^2_{n_r^{\text{PS}}} \triangleq (1-\rho)\sigma^2_{n_{a,r}} + \sigma^2_{n_{c,r}}$ is the variance of overall AWGN at the relay node, $n_r^{\text{PS}} \triangleq \sqrt{(1-\rho)}n_{a,d}(k) + n_{a,c}(k)$. Using (17), the SNR at the destination, γ_d^{PS}, in the PSR scheme is given by

$$\gamma_d^{\text{PS}} = \frac{\eta P_s |h|^2 |g|^2 \rho}{d_1^m d_2^m \sigma^2_{n_d}}, \tag{19}$$

In order to determine the throughput for the PSR scheme, we need to evaluate the ergodic capacity for source to relay link, C_r^{PS}, and for relay to destination link, C_d^{PS}. Using the received SNRs, γ_r^{PS} and γ_d^{PS}, defined in (18) and (19), respectively, C_r^{PS} and C_d^{PS} are given by

$$C_r^{\text{PS}} = \mathbb{E}_h\left\{\log_2(1+\gamma_R^{\text{PS}})\right\}\ ,\ C_d^{\text{PS}} = \mathbb{E}_{h,g}\left\{\log_2(1+\gamma_D^{\text{PS}})\right\} \tag{20}$$

where γ_R^{PS} depends on h and γ_D^{PS} depends on h and g. The analytical expressions for the ergodic capacities, C_r^{PS} and C_d^{PS}, are given in the following theorem.

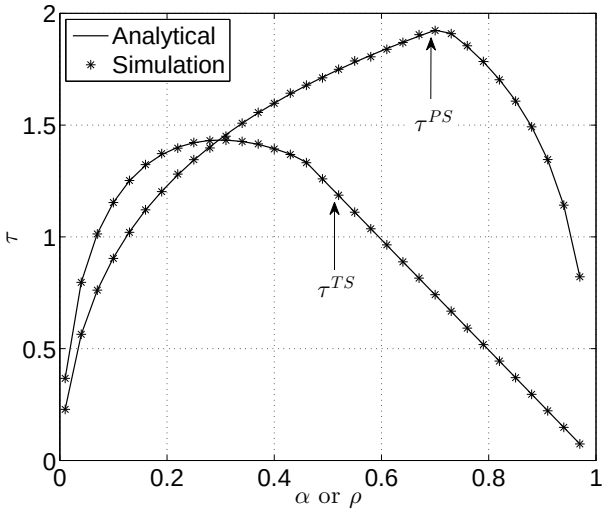

Fig. 3: Simulation based and analytical throughput at the destination node with respect to α for the TSR scheme and ρ for the PSR scheme.

Theorem 2. *The ergodic capacities, C_r^{PS} and C_d^{PS} for the PSR scheme are given by*

$$C_r^{PS} = \frac{\lambda_h e^{\frac{c}{\lambda_h}} E_1\left(\frac{c}{\lambda_h}\right)}{c\log(2)} \tag{21a}$$

$$C_d^{PS} = -\frac{2d}{\lambda_g \lambda_h \log(4)} G_{p,q}^{m,n}\left(\begin{matrix} [\{0\},\{\}] \\ [\{-1,0,0\},\{\}] \end{matrix} \middle| \frac{d}{\lambda_g \lambda_h} \right) \tag{21b}$$

where $c \triangleq \frac{d_1^m \sigma^2_{n_r^{PS}}}{P_s(1-\rho)}$, $d \triangleq \frac{d_1^m d_2^m \sigma^2_{n_d}}{\eta P_s \rho}$ and $E_1(x)$ and meijerG functions are defined in Theorem 1.

Proof: Theorem 2 can be proved by following the same steps as given in Appendix A. The details are omitted here for the sake of brevity. ■

Using (21), the ergodic capacity of the PSR scheme, C^{PS}, is given by

$$C^{\text{PS}} = \min\left\{C_r^{\text{PS}}, C_d^{\text{PS}}\right\} \tag{22}$$

Given that $T/2$ is the effective communication time from the source node to the destination node in the block of time T seconds and if source transmits at a fixed rate equal to the ergodic capacity, i.e., C^{PS} bits/sec/Hz, the throughput, τ^{PS} of the PSR scheme is given by

$$\tau^{\text{PS}} = \frac{T/2}{T}C^{\text{PS}} = \frac{1}{2}\min\left\{C_r^{\text{PS}}, C_d^{\text{PS}}\right\}, \tag{23}$$

where the throughput, τ^{PS} in (23) depends on P_s, η, ρ, d_1, d_2, $\sigma^2_{n_r^{\text{TS}}}$ and $\sigma^2_{n_d}$. It is desirable to find the optimal value of ρ, that result in the maximum value of throughput, τ^{PS}. Since, the analytical expression of τ^{PS} again involves complex meijerG function, which in turn depends on ρ, it seems intractable to evaluate the closed-form expressions for the optimal value of ρ in terms of τ. However, the optimization can be done offline by numerically evaluating the optimal values of α for the given system parameters, P_s, η, d_1, d_2, $\sigma^2_{n_r^{\text{PS}}}$ and $\sigma^2_{n_d}$.

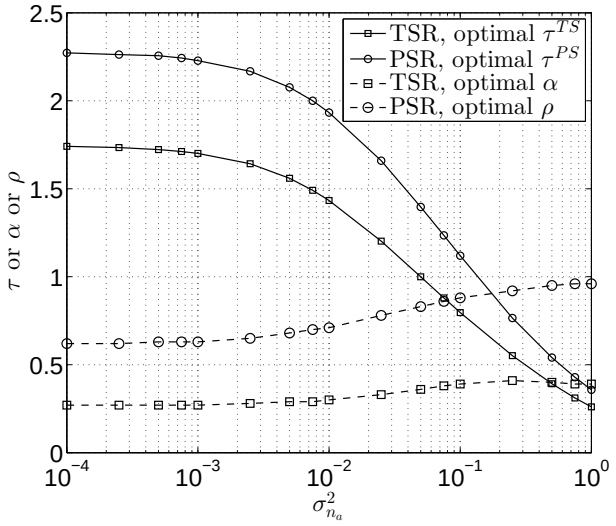

Fig. 4: Optimal throughput τ for the the TSR and the PSR schemes for different values of antenna noise variance $\sigma^2_{n_a}$ and $\sigma^2_{n_c} = 0.01$ (fixed)

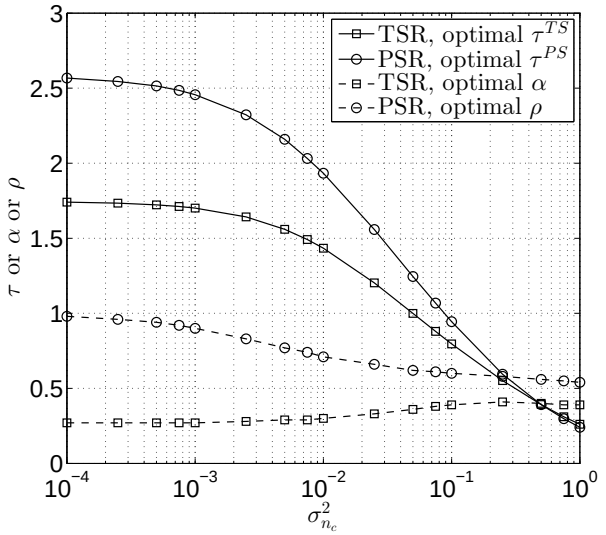

Fig. 5: Optimal throughput τ for the the TSR and the PSR schemes for different values of conversion noise variance $\sigma^2_{n_c}$ and $\sigma^2_{n_a} = 0.01$ (fixed)

V. Numerical Results

This section numerically analyzes the throughput performance of a DF relaying network in the presence of energy harvesting. We also use the derived analytical results to provide insights into the various design choices. The optimal value of throughput τ, optimal value of energy harvesting time α in the TSR scheme, and optimal value of power splitting ratio ρ in the PSR scheme are investigated for different values of the noise variances and the source to relay and the relay to destination distances, d_1 and d_2, respectively. Note that the optimal values of α and ρ are defined as the values, which result in the maximum throughput, τ^{TS} and τ^{PS}, respectively, at the destination node.

Unless otherwise stated, we set the energy harvesting efficiency, $\eta = 1$, source transmission power, $P_s = 1$ Joules/sec and path loss exponent $m = 2.7$. The distances d_1 and d_2 are normalized to unit value. For simplicity, similar noise variances at the relay and the destination nodes are assumed, i.e., antenna noise variance, $\sigma^2_{n_a} \triangleq \sigma^2_{n_{a,r}} = \sigma^2_{n_{a,d}}$ and conversion noise variance, $\sigma^2_{n_c} \triangleq \sigma^2_{n_{c,r}} = \sigma^2_{n_{c,d}}$. The mean values, λ_h and λ_g, of the exponential random variables $|h|^2$ and $|g|^2$, respectively, are set to 1.

Fig. 3 plots the analytical and simulation based results of throughput, τ^{TS} and τ^{PS}, with respect to α and ρ, for the TSR and PSR schemes, respectively. Note that the analytical throughput results depend on the analytical expressions of ergodic capacity in (9) and (21). However, the simulation results depend on the simulation based expressions for ergodic capacity in (8) and (20), which are evaluated by averaging these expressions over 10^5 random realizations of the Rayleigh fading channels h and g. Fig. 3 shows that analytical results of throughput perfectly matches with the simulation results for the different values of α and ρ for the TSR and PSR schemes, respectively. This verifies our analysis in Theorem 1 and Theorem 2. Fig. 3 also shows that for the chosen system parameters, the maximum throughput in the PSR scheme is greater than the maximum throughput achievable in the TSR scheme.

Fig. 4 plots the optimal throughput τ for the TSR and the PSR schemes for different values of antenna noise variance, $\sigma^2_{n_a}$, while keeping the conversion noise fixed at $\sigma^2_{n_c} = 0.01$. On the other hand, Fig. 4 plots the optimal throughput τ for the TSR and the PSR schemes for different values of conversion noise variance, $\sigma^2_{n_c}$, while keeping the antenna noise fixed at $\sigma^2_{n_a} = 0.01$. Fig. 4 shows that the PSR scheme outperforms the TSR scheme for different considered values of noise variance, $\sigma^2_{n_a}$. On the other hand, Fig. 5 shows that there is a cross over between the performances of the TSR and PSR schemes at the value of noise variance, $\sigma^2_{n_c} = 0.5$.

Fig. 4 and Fig. 5 also plot the optimal values of α and ρ for the TSR and the PSR schemes, for different values of $\sigma^2_{n_a}$ (Fig. 4) and $\sigma^2_{n_c}$ (Fig. 5). Fig. 4 and Fig. 5 show that the optimal value of α increases by increasing $\sigma^2_{n_a}$ or $\sigma^2_{n_c}$. However, the optimal ρ increases by increasing $\sigma^2_{n_a}$ (see Fig. 4) and decreases by increasing $\sigma^2_{n_c}$ (see Fig. 5). This is due to the fact that for the TSR scheme, both noise processes, the antenna noise at the baseband $n_{a,r}(k)$ and the conversion noise $n_{c,r}(k)$, affect the received signal $y_r(k)$ in the same way. Consequently, the trend for the optimal value of α is same when plotted with respect to the noise variances, $\sigma^2_{n_a}$ or $\sigma^2_{n_c}$, in Fig. 4 and Fig. 5, respectively. On the other hand, for the PSR scheme, the baseband antenna noise $n_{a,r}(k)$ affects the received signal $y_r(k)$ and the conversion noise $n_{c,r}(k)$ affects the portion of the received signal strength, $\sqrt{1-\rho}y_r(t)$. As a result, the trend for the optimal value of ρ is different when plotted with respect to the noise variances, $\sigma^2_{n_a}$ or $\sigma^2_{n_c}$, in Fig. 4 and Fig. 5, respectively.

VI. Conclusions

In this paper, a DF relaying network has been considered, where an energy constrained relay node harvests energy from the received RF signal and uses that harvested energy to forward the source signal to the destination node. To enable wireless energy harvesting and information processing at the relay, both TSR and PSR schemes have been considered. The exact achievable throughput at the destination is determined by deriving the ergodic

capacity of a DF relaying network in the presence of wireless energy harvesting constraint at the relay node. The optimal value of energy harvesting time in the TSR protocol and the optimal value of power splitting ratio in the PSR protocol are numerically investigated. The numerical analysis in this paper has provided practical insights into the effect of various system parameters on the performance of wireless energy harvesting and information processing using DF relay nodes.

APPENDIX A
PROOF OF THEOREM 1 IN (9)

Let us first find the analytical expression for C_r^{TS}. Using (8), C_r^{TS} is given by

$$C_r^{\text{TS}} = \int_{\gamma=0}^{\infty} f_{\gamma_r^{\text{TS}}}(\gamma) \log_2(1+\gamma) d\gamma \tag{A.1}$$

where $f_{\gamma_r^{\text{TS}}}(\gamma)$ is the probability density function (PDF) of γ_r^{TS} in (6). Since $|h|^2$ is exponentially distributed, γ_r^{TS} is also exponentially distributed, i.e., $f_{\gamma_r^{\text{TS}}}(\gamma) = \frac{a}{\lambda_h} e^{-\frac{a\gamma}{\lambda_h}}$, where $a \triangleq \frac{d_1^m \sigma_{n_r^{\text{TS}}}^2}{P_s}$. Substituting the value of $f_{\gamma_r^{\text{TS}}}(\gamma)$ into (A.1), C_r^{TS} is given by

$$C_r^{\text{TS}} = \int_{\gamma=0}^{\infty} \frac{a}{\lambda_h} e^{-\frac{a\gamma}{\lambda_h}} \log_2(1+\gamma) d\gamma = \frac{\lambda_h e^{\frac{a}{\lambda_h}} E_1\left(\frac{a}{\lambda_h}\right)}{a \log(2)}, \tag{A.2}$$

where $E_1(x) = \int_x^{\infty} \frac{e^{-t}}{t} dt$ is the exponential integral. Next, using (8), C_d^{TS} is given by

$$C_d^{\text{TS}} = \int_{\gamma=0}^{\infty} f_{\gamma_d^{\text{TS}}}(\gamma) \log_2(1+\gamma) d\gamma \tag{A.3}$$

where $f_{\gamma_d^{\text{TS}}}(\gamma)$ is the PDF of γ_d^{TS} in (7). In order to find the PDF of γ_d^{TS}, let us first find the cumulative distribution function (CDF), $F_{\gamma_d^{\text{TS}}}(\gamma)$ of γ_d^{TS}, which is given by

$$F_{\gamma_d^{\text{TS}}}(\gamma) = p\left(\gamma_d^{\text{TS}} < \gamma\right) \tag{A.4a}$$

$$= p\left(|g|^2 < \frac{b\gamma}{|h|^2}\right) \tag{A.4b}$$

$$= \int_{x=0}^{\infty} f_{|h|^2}(x) \left(1 - e^{-\frac{b\gamma}{x\lambda_g}}\right) dx \tag{A.4c}$$

$$= 1 - \sqrt{\frac{4b\gamma}{\lambda_g \lambda_h}} K_1\left(\sqrt{\frac{4b\gamma}{\lambda_g \lambda_h}}\right) \tag{A.4d}$$

where $b \triangleq \frac{d_1^m d_2^m \sigma_{n_d}^2 (1-\alpha)}{2\eta P_s \alpha}$, $f_{|h|^2}(x) = \frac{1}{\lambda_h} e^{-\frac{x}{\lambda_h}}$ is the PDF of exponential random variable $|h|^2$, (A.4c) follows from (A.4b) because $|g|^2$ is exponential random variable with mean λ_g, $K_1(\cdot)$ is the first-order modified Bessel function of the second kind [18], and (A.4d) follows from (A.4c) by using the formula, $\int_0^{\infty} e^{-\frac{\beta}{4x} - \gamma x} dx = \sqrt{\frac{\beta}{\gamma}} K_1(\sqrt{\beta\gamma})$ [18, §3.324.1]. By taking the derivative of the CDF function, $F_{\gamma_d^{\text{TS}}}(\gamma)$, $f_{\gamma_d^{\text{TS}}}(\gamma)$ is given by

$$f_{\gamma_d^{\text{TS}}}(\gamma) = \frac{\partial F_{\gamma_d^{\text{TS}}}(\gamma)}{\partial \gamma} = \frac{2b}{\lambda_g \lambda_h} K_0\left(\sqrt{\frac{4b\gamma}{\lambda_g \lambda_h}}\right) \tag{A.5}$$

where we used the property of bessel function, $\frac{d}{dz}\left(z^v K_v(z)\right) = -z^v K_{v-1}(z)$ [18, §8.486.18]. Substituting the value of $f_{\gamma_d^{\text{TS}}}(\gamma)$ from (A.5) into (A.3), C_d^{TS} is given by

$$C_d^{\text{TS}} = \int_{\gamma=0}^{\infty} \frac{2b}{\lambda_g \lambda_h} K_0\left(\sqrt{\frac{4b\gamma}{\lambda_g \lambda_h}}\right) \log_2(1+\gamma) d\gamma$$

$$= -\frac{2b}{\lambda_g \lambda_h \log(4)} G_{p,q}^{m,n}\left(\begin{matrix} [\{0\},\{\}] \\ [\{-1,0,0\},\{\}] \end{matrix} \middle| \frac{b}{\lambda_g \lambda_h} \right), \tag{A.6}$$

where the meijerG function $G_{p,q}^{m,n}\left(\begin{matrix} a_1,\ldots,a_p \\ b_1,\ldots,b_q \end{matrix} \middle| z \right)$ is defined in (10). This ends the proof of Theorem 1.

REFERENCES

[1] X. Zhou, R. Zhang, and C. K. Ho, "Wireless information and power transfer: Architecture design and rate-energy tradeoff," in *Proc. IEEE GLOBECOM*, 2012.

[2] S. H. Lee, R. Zhang, and K. B. Huang, "Opportunistic wireless energy harvesting in cognitive radio networks," *to appear in IEEE Trans. Wireless Commun.*, 2013. [Online]. Available: http://arxiv.org/abs/1302.4793

[3] L. Liu, R. Zhang, and K.-C. Chua, "Wireless information transfer with opportunistic energy harvesting," *IEEE Trans. Wireless Commun.*, vol. 12, no. 1, pp. 288–300, Jan. 2013.

[4] L. Liu, R. Zhang, and K. C. Chua, "Wireless information and power transfer: a dynamic power splitting approach," *to appear in IEEE Trans. Commun.*, 2013. [Online]. Available: http://arxiv.org/abs/1302.0585

[5] R. Zhang and C. K. Ho, "MIMO broadcasting for simultaneous wireless information and power transfer," *IEEE Trans. Wireless Commun.*, vol. 12, no. 5, pp. 1989–2001, May 2013.

[6] J. Park and B. Clerckx, "Joint wireless information and energy transfer in a two-user MIMO interference channel," *IEEE Trans. Commun.*, vol. 12, no. 8, pp. 4210–4221, Aug. 2013.

[7] D. W. K. Ng, E. S. Lo, and R. Schober, "Energy-efficient resource allocation in multiuser ofdm systems with wireless information and power transfer," in *Proc IEEE WCNC*, 2013.

[8] Z. Xiang and M. Tao, "Robust beamforming for wireless information and power transmission," *IEEE Wireless Commun. Letters*, vol. 1, no. 4, pp. 372–375, 2012.

[9] D. W. K. Ng, L. Xiang, and R. Schober, "Multi-objective beamforming for secure communication in systems with wireless information and power transfer," in *Proc IEEE PIMRC*, 2013.

[10] B. Medepally and N. B. Mehta, "Voluntary energy harvesting relays and selection in cooperative wireless networks," *IEEE Trans. Wireless Commun.*, vol. 9, no. 11, pp. 3543–3553, Nov. 2010.

[11] B. K. Chalise, Y. D. Zhang, and M. G. Amin, "Energy harvesting in an OSTBC based amplify-and-forward MIMO relay system," in *Proc. IEEE ICASSP*, 2012.

[12] K. Ishibashi, H. Ochiai, and V. Tarokh, "Energy harvesting cooperative communications," in *Proc. IEEE PIMRC*, 2012.

[13] A. M. Fouladgar and O. Simeone, "On the transfer of information and energy in multi-user systems," *IEEE Commun. Lett.*, vol. 16, no. 11, pp. 1733–1737, Nov. 2012.

[14] I. Krikidis, S. Timotheou, and S. Sasaki, "RF energy transfer for cooperative networks: Data relaying or energy harvesting?" *IEEE Commun. Lett.*, vol. 16, no. 11, pp. 1772–1775, 2012.

[15] A. A. Nasir, X. Zhou, S. Durrani, and R. A. Kennedy, "Relaying protocols for wireless energy harvesting and information processing," *IEEE Trans. Wireless Commun.*, vol. 12, no. 7, pp. 3622–3636, Jul. 2013.

[16] Z. Ding, S. M. Perlaza, I. Esnaola, and H. V. Poor, "Power allocation strategies in energy harvesting wireless cooperative networks," *ArXiv Technical Report*, 2013. [Online]. Available: http://arxiv.org/abs/1307.1630

[17] Y. Sun, X. Zhong, X. Chen, S. Zhou, and J. Wang, "Ergodic capacity of decode-and-forward relay strategies over general fast fading channels," *IEEE Electronics Letters*, vol. 47, no. 2, pp. 148–150, Jan. 2011.

[18] I. S. Gradshteyn and I. M. Ryzhik, *Table of integrals, series, and products*, 4, Ed. Academic Press, Inc., 1980.